CHAPTER 3

MATERIALS AND METHODS

3.1 Materials

The present study required a number of materials that include chemicals and reagents, equipments, food samples, and softwares.

3.1.1 Chemicals and reagents

The chemicals and reagents used were Ethylene-diamine-tetra-acetic (EDTA) acid, trichloroacetic acid (TCA), sodium chloride (NaCl), hydrogen peroxide (H_2O_2), pyrogallol, phenolphthalein indicator 2,6-dichloroindophenol, sodium phosphate monobasic, sodium phosphate dibasic, polyvinylpolypyrrolidone (PVPP), pyrocatechol, nutrient agar, cysteine, triton X-100, casein, glycine, metaphosphoric acid, sugar, sodium hydroxide, and sodium bicarbonate. All the chemicals and reagents were of analytical grade.

3.1.2 Machines and equipments

A lab-scale continuous ohmic heating (COH) system that consisted of Teflon chamber, platinized titanium electrodes, K-type thermocouple (Make: Thermonic, Model: K-C-2M), Teflon tape, variac transformer (0-500 V, 1ϕ, 50 Hz) (Make: Servokon Systems Ltd., Model: D.500), temperature controller (Make: Multispan, Model: UTC 4202), peristaltic pump (Make: Enertech Electronics Pvt. Ltd., Model: ENPD 100 Victor), multimeter (Make: Fluke, Model: 115 True RMS). The other equipment used in the study was a vacuum oven (Make: Jeio Tech, Model: OV-11), weighing balance (Make: Mettler Toledo, Model: ME204), pH meter (Make: Eutech Instruments, Model: pH 700), electrical conductivity meter (Make: Eutech Instruments, Model: CON700), refractometer (range = 0-32 °Brix) (Make: ERMA, Model: ERB-32), Hunter Colour Lab Spectrophotometer (Make: Hunter Colour Lab USA, Model: Ultrascan VIS), UV-VIS spectrophotometer (Make: Dynamica, Model: HALO DB-20S), BOD incubator (Make: Impact Icon Instruments Company, Model: 11C 109), laminar flow (Model: Impact Icon Instruments Company, Model: 11C 124-18), hot water bath (Make: Riviera Glass Pvt. Ltd., Model: 50191000), fruit juicer (Make: Gee Gee (Food & Packaging) Co. (P) Ltd.), vortex shaker (Make: Labquest Borosil, Model: bhrmi 1.0).

3.1.3 Food samples

Fresh fruits like cucumber, tomato, orange, pineapple, and lemon were purchased from the local market of Tezpur University, Assam, India. The fruit juice was prepared (Section 3.2.3) and used to test the heating performance of the developed COH system. Further, the thermal processing of pineapple juice using the COH system for its quality parameters were explored.

3.1.4 Softwares

Design Expert 7.1, Microsoft Office 2019, SPSS 23.0, and MATLAB R2015a were used for the experimental analysis.

3.2 Methodologies

The overall methodology of the present work is summarised in the flow chart as shown in Fig. 3.1. The entire work comprised five objectives, starting with the design and development of a COH cell and its performance evaluation with different fruit juices. It was then followed by the standardization of pineapple juice to study COH behaviour followed by the development of an isothermal holding chamber for the standardized pineapple juice (22 °Brix/Acid). Further, the effect of COH treatment on enzyme and microbial inactivation and physico-chemical parameters were studied and the process parameters were optimized. The kinetic modelling of the enzyme and microbial inactivation and vitamin C degradation was studied.

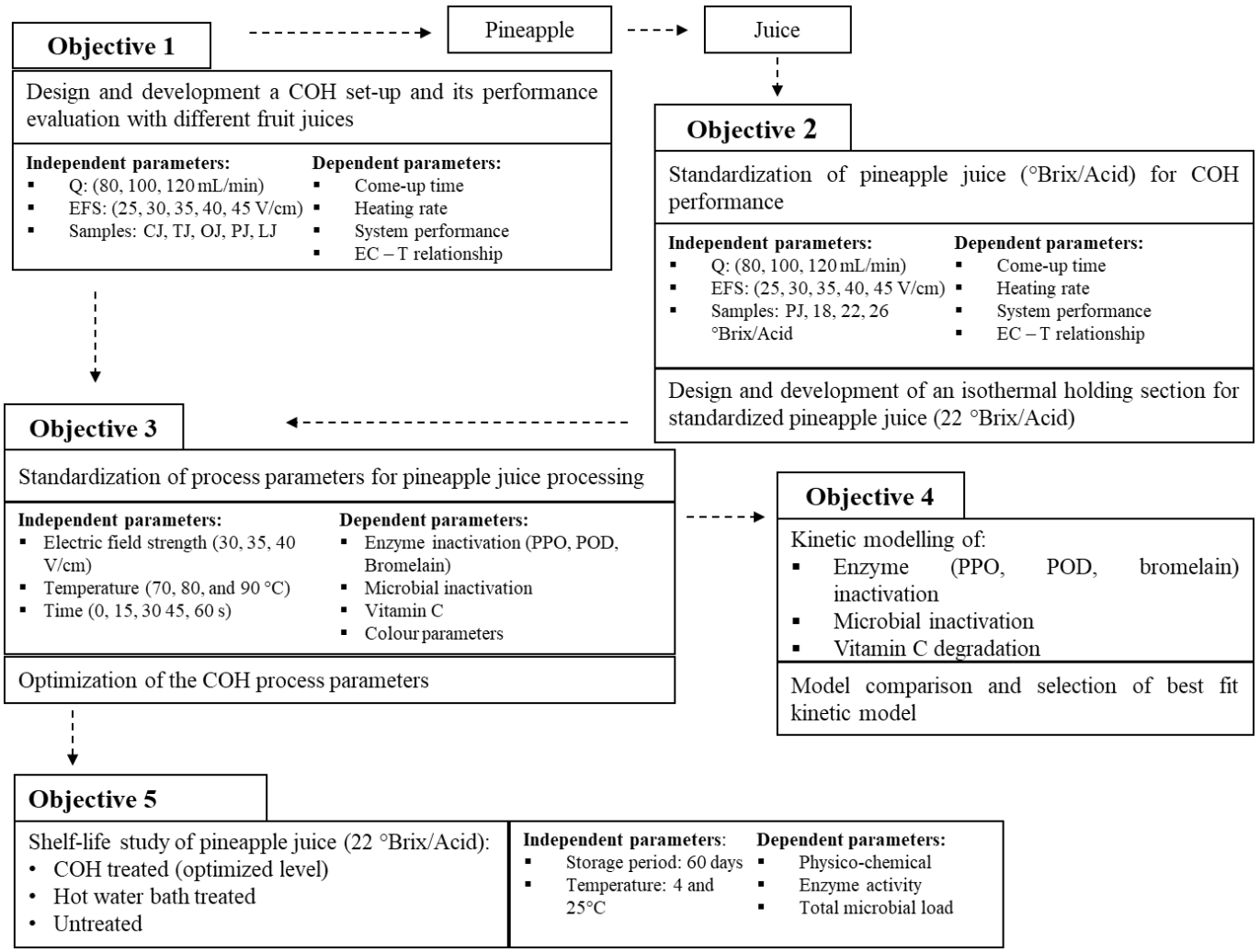

Fig. 3.1 Overall flow chart of the work. Where CJ, TJ, OJ, PJ, and LJ are cucumber, tomato, orange, pineapple, and lemon juice, respectively. Also, Q, EFS, EC, and T are flow rate, electric field strength, electrical conductivity, and temperature, respectively

Finally, the storage study of optimized COH-treated pineapple juice was compared with conventional treated and untreated pineapple juice. The detailed objective wise methodology is summarised in the flow chart in section 3.2.1.

3.2.1 Objective wise methodologies and flow chart

3.2.1.1 Objective 1: To develop a lab-scale continuous ohmic heating system and its performance evaluation with different fruit juices

A lab-scale COH cell was developed, which consisted of a cylindrical Teflon chamber equipped with two platinized titanium electrodes placed at both ends. The details of the design and development of the COH system are explained in section 3.2.2.

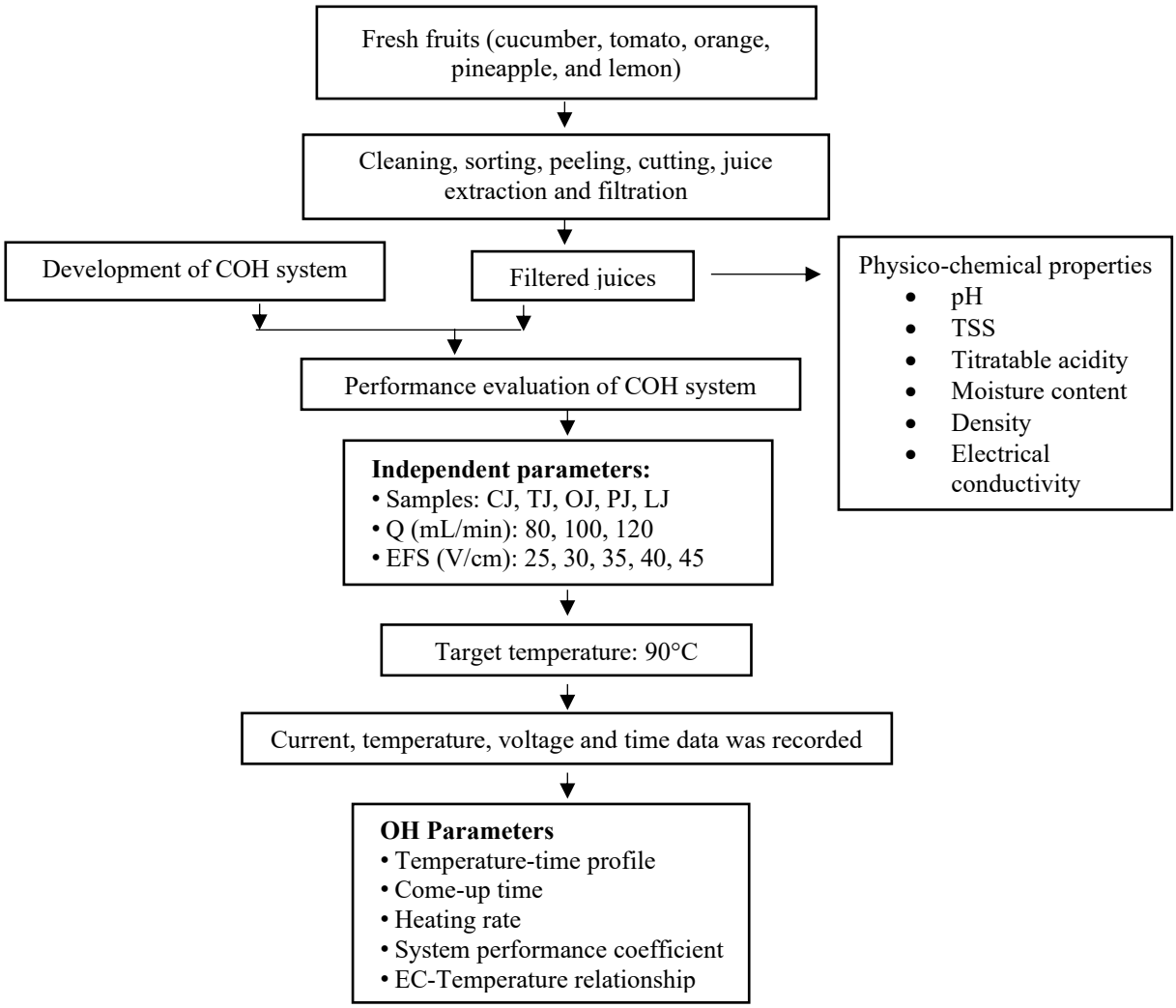

Fig. 3.2 Flow chart of the objective 1. Where CJ, TJ, OJ, PJ, and LJ are cucumber, tomato, orange, pineapple, and lemon juice, respectively. Also, Q, EFS, and EC are flow rate, electric field strength, and electrical conductivity, respectively

The juice was pumped to the COH chamber from the inlet storage tank through a peristaltic pump. The treatment chamber was filled entirely with juice before the electric power supply to

avoid any air pockets within the treatment chamber. The juice was heated until the target temperature of 90 °C was achieved. A full factorial design was used to conduct experiments with independent variables of EFS (25, 30, 35, 40, and 45 V/cm), flow rate (80, 100, and 120 mL/min), and fruit juices (cucumber, tomato, orange, pineapple, and lemon). The ohmic parameters like temperature-time profile, come-up time (CUT), heating rate (HR), system performance coefficient (SPC), and electrical conductivity-temperature (EC-T) relationship of different fruit juices were studied as shown in Fig. 3.2.

3.2.1.2 Objective 2: To standardize pineapple juice (°Brix/Acid) for continuous ohmic heating performance

Fresh pineapple juice was standardized at different °Brix/Acid (18, 22, and 26 °Brix/Acid) and used to study the heating performance of the COH system.

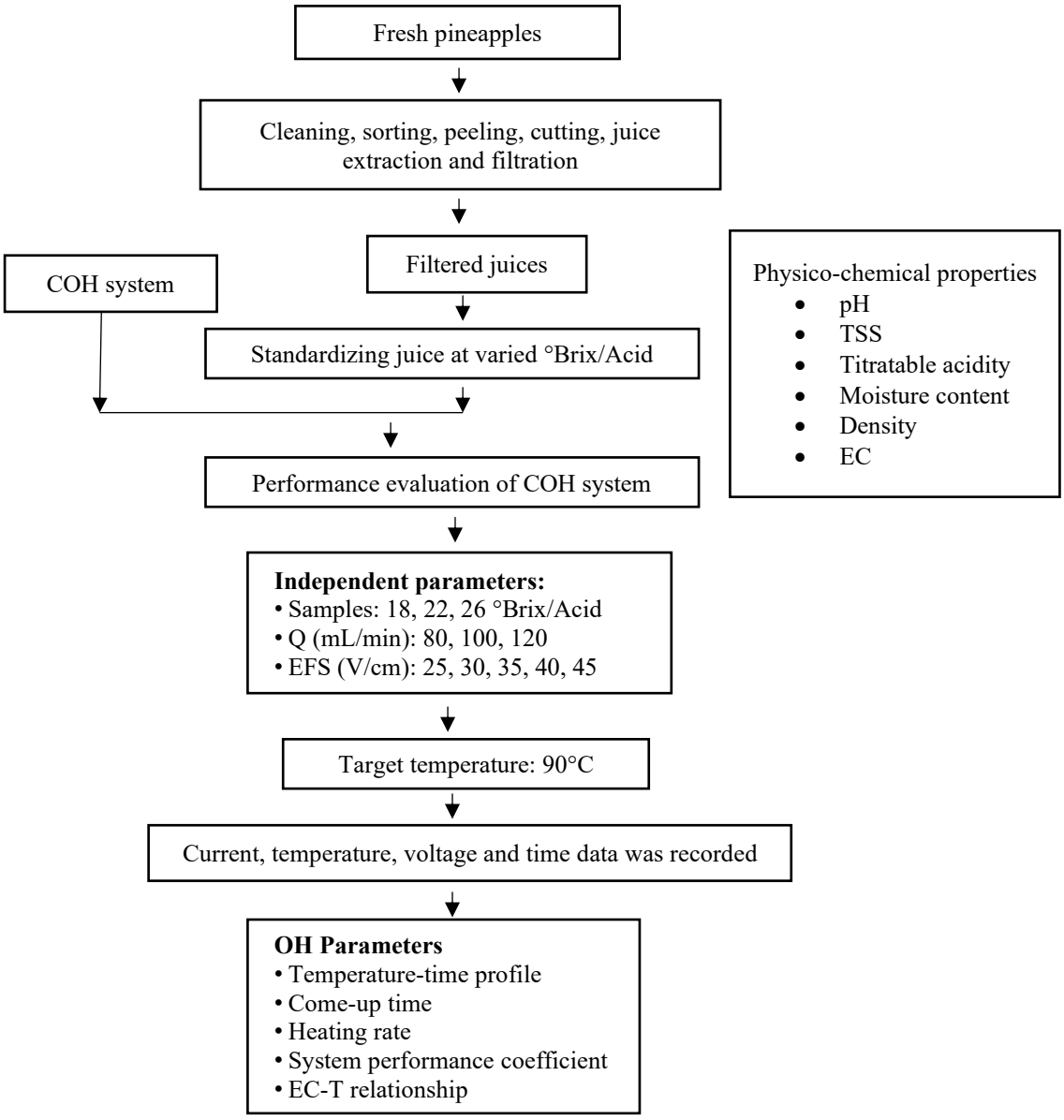

Fig. 3.3 Flow chart of the objective 2

The detailed procedure for juice standardization is explained in section 3.2.5. A similar procedure was used to conduct the experiments, as explained in section 3.2.1.1. The results of standardized pineapple juice were compared with the unstandardized pineapple juice. The detailed plan of the work is shown in Fig. 3.3.

Further, an isothermal holding chamber was designed and developed for the standardized pineapple juice (22 °Brix/Acid) to hold juice for 0, 15, 30, 45, and 60 s, respectively, for each EFS – temperature combination (EFS: 30, 35, 40 V/cm; Temperature: 70, 80, 90 °C) to study the effect of COH treatment on enzyme and microbial inactivation, vitamin C, and colour. For this, the mass flow rate of the juice was determined using a trial and iterative approach to achieve a steady temperature of 70, 80, and 90 °C, respectively, for EFS 30, 35, and 40 V/cm. The details are explained in section 3.2.2.

3.2.1.3 Objective 3: To standardize the process parameters for thermal processing of pineapple juice by continuous ohmic heating

Fresh pineapple juice was extracted from matured pineapples and was standardized to 22 °Brix/Acid. The juice was immediately treated in the lab-scale COH system under different EFS (30, 35, and 40 V/cm), temperature (70, 80, and 90 °C), and holding time (0, 15, 30, 45, and 60 s). A full factorial design was used to conduct the experiments. The sampling was done at the outlet port of the COH heating cell and the outlet port of the isothermal holding chamber. The sample was immediately cooled in an ice bath and used for analysis, including enzyme inactivation (polyphenol oxidase (PPO), peroxidase (POD), and bromelain), total microbial inactivation, vitamin C retention, and colour parameters. Further, the obtained data was used to optimize the process parameters. The detailed plan of the work is shown in Fig. 3.4.

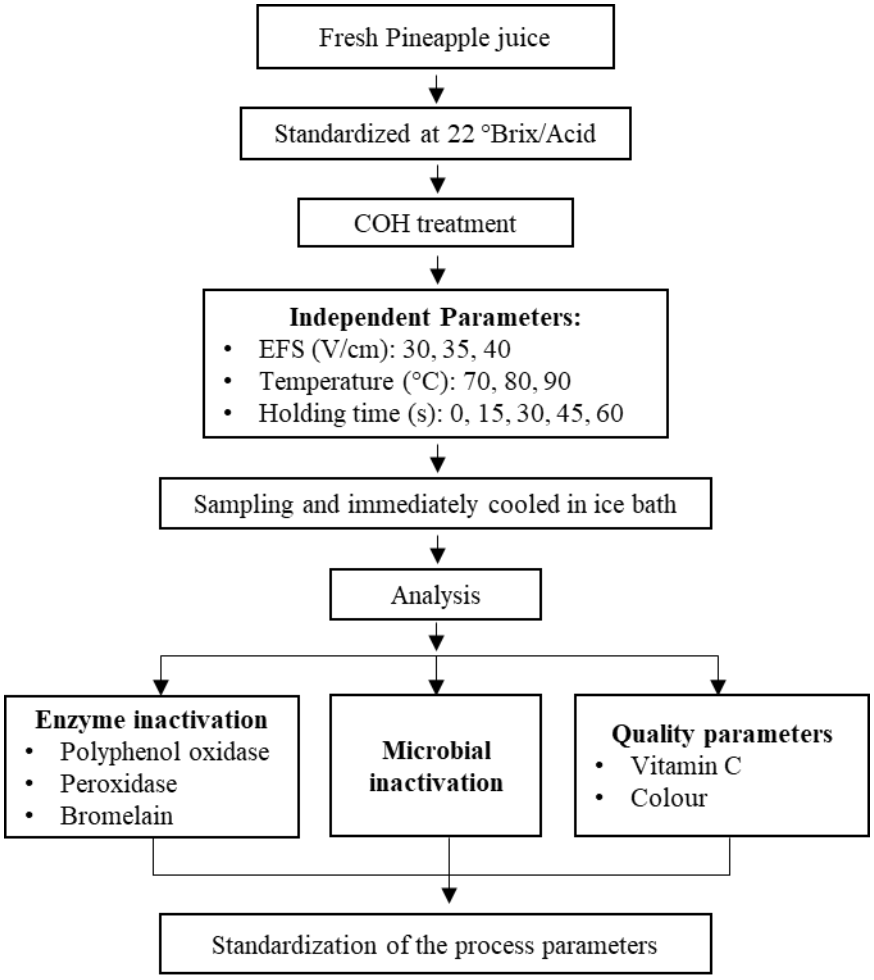

Fig. 3.4 Flow chart of objective 3

3.2.1.4 Objective 4: To model inactivation kinetics of enzymes, microbes, and quality attributes during continuous ohmic heating of pineapple juice.

The inactivation kinetic modelling of PPO, POD, bromelain, microbial, and vitamin C degradation was done using the experimental data of objective 3. The detailed plan of the work is shown in Fig. 3.5. PPO and POD inactivation kinetic modelling was done using first order, Weibull distribution, sigmoidal logistic, distinct isozymes, and fractional conversion model. For bromelain inactivation and vitamin C degradation, first-order, Weibull distribution, and Logistic models were employed. Also, to study microbial inactivation kinetic, first order, modified Gompertz, and Weibull distribution models were used. Model parameters were analysed, and the best fit kinetic model was selected for each response parameter (PPO, POD, bromelain, microbial, and vitamin C) based on statistical parameters like high coefficient of determination (R^2), low sum of square error (SSE), low root mean square error (RMSE), and low residuals. The accuracy factor (A_f) and bias factor (B_f) were also studied for the validation

and performance capabilities of the different models. It is reasonable that sometimes several models fit equally well in a given dataset, and these datasets do not support selecting one model. For this, Akaike information criteria (AIC) Akaike increment (Δ_i) values were used to discriminate, rank, and choose the best model among several competing models.

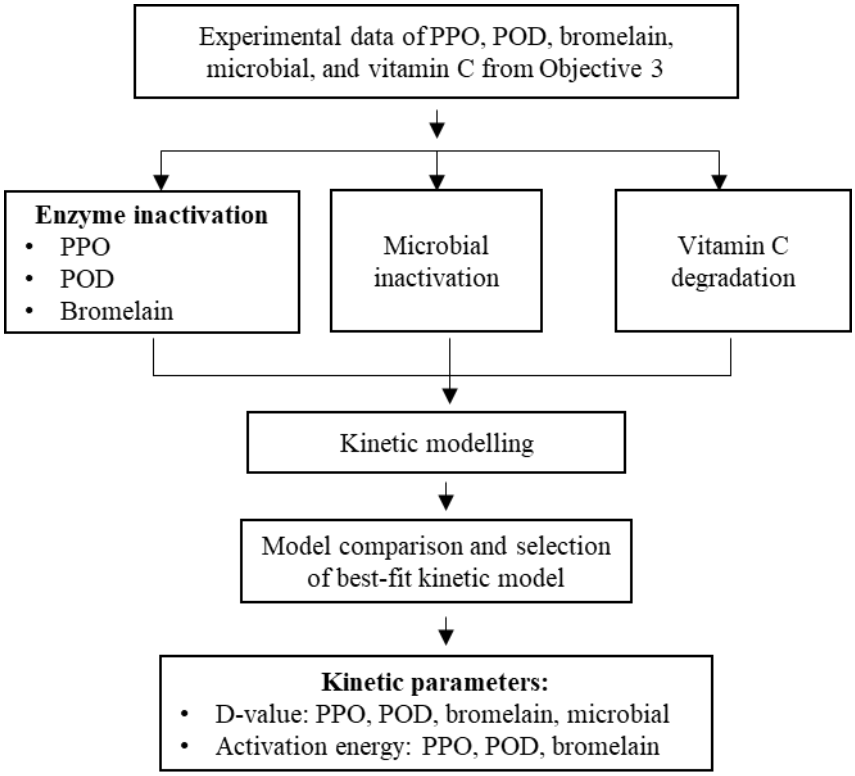

Fig. 3.5 Flow chart of objective 4

3.2.1.5 Objective 5: To study the shelf-life of continuous ohmic heat-treated pineapple juice under different storage conditions.

Fresh pineapple juice was standardized to 22 °Brix/Acid and used immediately for COH (EFS = 40 V/cm; T = 90 °C; t = 60 s) and conventional water bath (T = 90 °C; t = 60 s) treatment. The detailed plan of the work is shown in Fig. 3.6. The sampling was done in 20 mL pre-sterilised vial glasses in a pre-sterilised environment. For conventional water bath treatment, the juice was first sampled in sterilised vial glasses and sealed, and then the thermal treatment was provided to restrict the recontamination of the samples. The samples were stored at two different temperatures (4 °C and 25 °C). Physico-chemical parameters (pH, TSS, titratable acidity, vitamin C, electrical conductivity, and colour), enzyme activity (PPO, POD, and bromelain), and microbial growth were examined regularly.

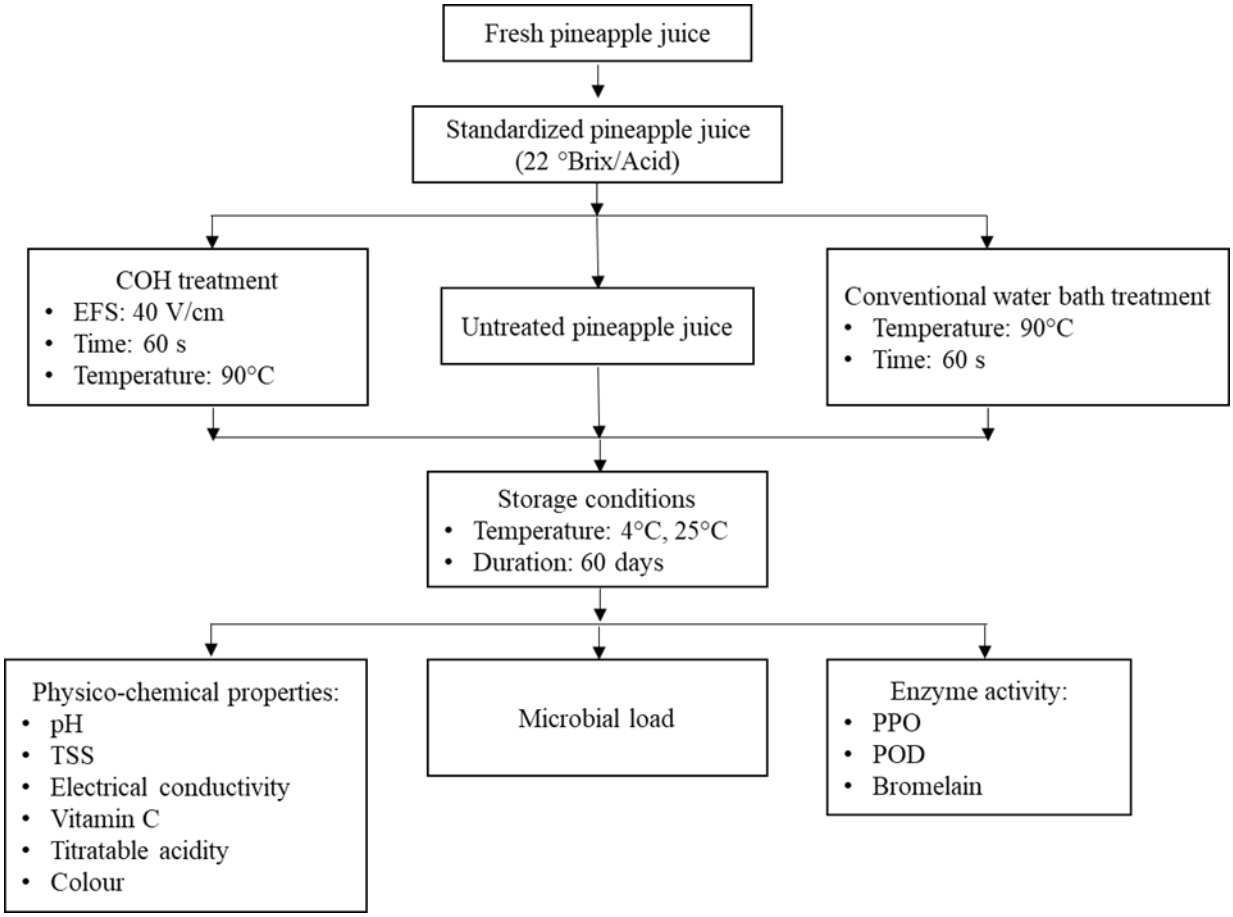

Fig. 3.6 Flow chart of objective 5

3.2.2 Design and development of continuous ohmic heating (COH) system

3.2.2.1 Design requirements

The COH system should fulfil the following requirements:

i. There should be no/minimal electrochemical reactions at the electrode/samples interface.
ii. The electrode should be corrosion-resistant.
iii. The system should be compatible with an input power supply of 220 V and 50 Hz.
iv. The system should be able to provide an electric field in the range of 10-45 V/cm.
v. The system must be capable of measuring current, voltage, and temperature (PID control).
vi. The system should also have an isothermal holding section to meet the requirement of thermal treatment.
vii. The system must be capable of a metered continuous flow of fruit juice using a peristaltic pump.

viii. The heating and holding section should not be an electric conductor to avoid any chance of a short circuit.

ix. The heating and holding section should not be a thermal conductor to avoid any heat loss.

x. The system must be able to handle/process different fruit juices.

xi. The system must be easy to dismantle for regular cleaning and hygiene.

3.2.2.2 Conceptual design

The COH system was developed in two stages:

i. Development of a COH heating chamber

ii. Development of an isothermal holding chamber

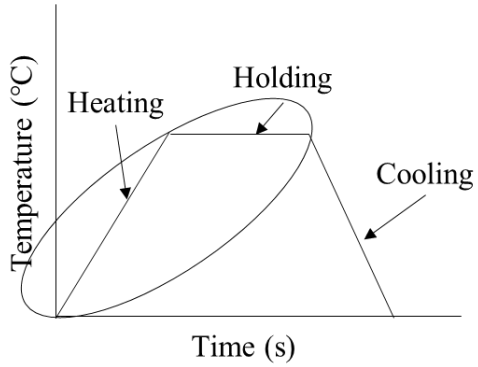

Fig. 3.7 Steps in thermal treatment of fruit juice

Any thermal processing of fruit juices involves basically three steps, viz., heating, holding, and cooling, as shown in Fig. 3.7. Conventional way of heating causes non-homogeneity of heat transfer and resulting a more significant temperature gradient within the food matrix. This causes an uneven processing of fruit juices and takes longer overall processing time. The conceptual design was to replace the conventional mode of heating with ohmic heating followed by isothermal holding. The COH system was designed with the aim of heating the electrically conductive fruit juices by the principle of joule heating. The heating and holding chambers were cylindrical in shape and made of Teflon material.

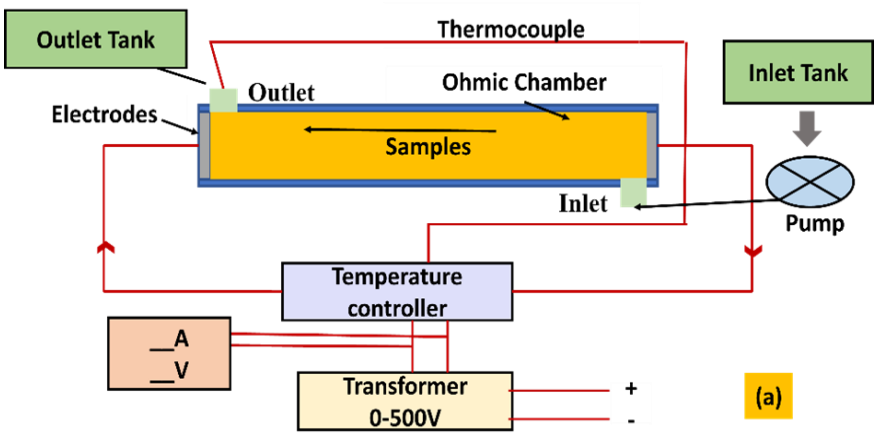

Fig. 3.8 Schematic design of a lab-scale COH chamber

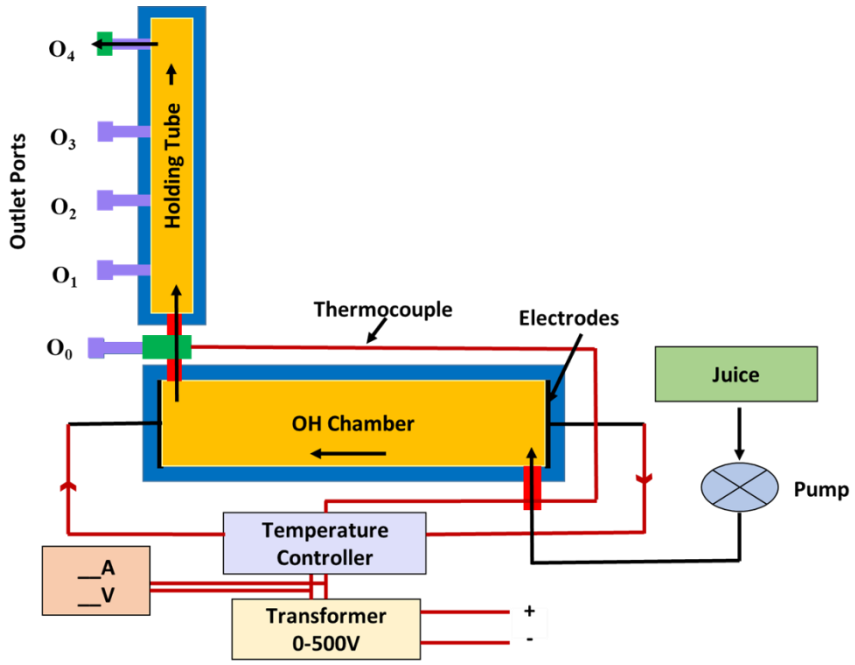

Fig. 3.9 Schematic design of a lab-scale COH chamber equipped with an isothermal holding chamber

Two electrodes were fixed at both ends of the heating chamber and enclosed with two detachable lids in such a way that there was sufficient space between them to heat the fruit juice samples. Two ports, viz., an input and an output port, were made at the two ends of the heating chamber in opposite directions, lying within the space between two electrodes for the juice to flow continuously from the input port and come out from the output port. A thermocouple was inserted at the outlet port of the heating chamber to measure the temperature of the outgoing juice. The electrical circuit was completed by supplying electric voltage across the electrodes through a variac transformer. The fruit juice in between the two electrodes gets

heated due to the resistance to the flow of electric current following the joules law. The electric field was controlled by a variac transformer to set and provide a desired electric field strength across the fruit juice. The cool fruit juice was pumped to the heating chamber by a peristaltic pump through the inlet port, was heated up ohmically, and then went to the isothermal holding chamber via the outlet port of the heating chamber. The isothermal holding chamber holds the ohmically heated fruit juice up to a certain period, and then it comes out through the outlet port of the holding chamber. The main idea is to provide the temperature-time combination for the thermal treatment of the fruit juice. The complete COH set-up was made leak proof. Temperature, current, and voltage data were recorded. The schematic design of a lab-scale COH chamber is shown in Fig. 3.8 and a COH chamber equipped with an isothermal holding chamber is shown in Fig. 3.9.

3.2.2.3 Design and fabrication of COH set-up

Based on the conceptual design, a lab-scale COH system was developed. The developed system consisted of the following components:

i. Heating chamber
ii. Holding chamber
iii. Electrodes
iv. T-shaped jointer port
v. Power supply and temperature controller
vi. Other accessories

3.2.2.3.1 Heating chamber

The heating chamber was made with Teflon material and the shape was hollow cylindrical. The Teflon was chosen as it was reported to be a good insulating material for heat and current and found application in many industrial set-ups. The inner and outer diameters of the heating chamber were 48 and 75 mm, respectively. Two detachable lids were used to fix the electrodes at both ends of the hollow heating chamber. The lids get easily fastened with spiral thread joints over the length of 10 mm from either end of the hollow heating chamber. The overall length of the heating chamber, including two detachable cover lids on both ends, was 131 mm, while the actual working length of the heating chamber where the fruit juices get heated is 100 mm. The detachable lids were also made of Teflon material to restrict the heat loss as well as to make the heating chamber completely electric insulated. For the juice to flow continuously, two ports, viz., one for inlet and the other for outlet opening, were made at both ends of the heating chamber in opposite directions. The design dimensions of the heating chamber are shown in

Table 3.1, and its schematic diagram is shown in Fig. 3.10. The joints and openings were fastened using Teflon tape to make it leakage-proof during ohmic heating operations.

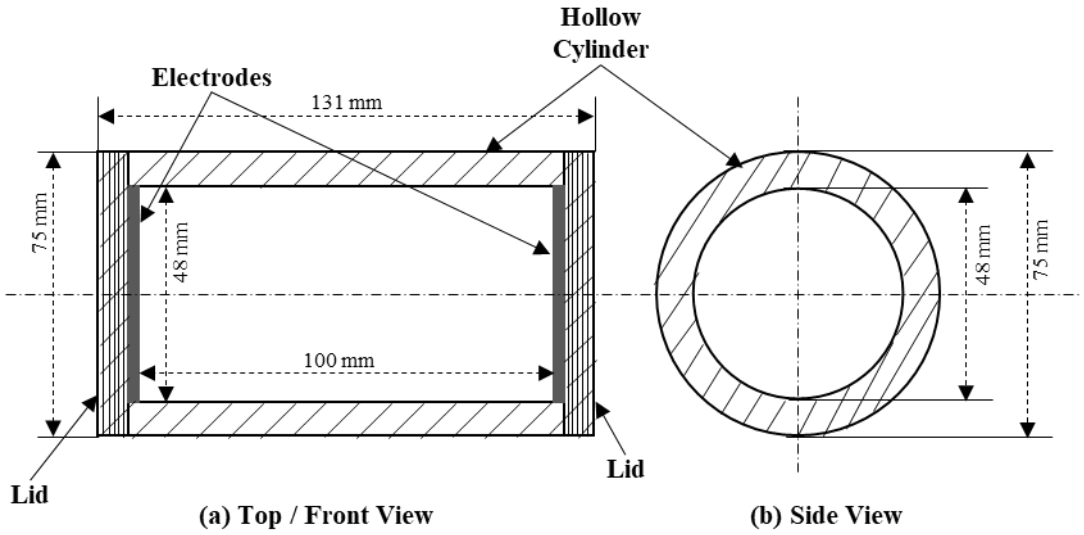

Fig. 3.10 Schematic diagram of a heating chamber

3.2.2.3.2 Holding Chamber

The isothermal holding chamber was made with Teflon material and the shape was hollow cylindrical. The inner and outer diameters of the chamber were 23 mm and 51 mm, respectively. Two detachable lids were fastened with spiral thread at both ends over a length of 10 mm. The bottom end lid, i.e. facing the heating chamber, acted as the input port to the isothermal chamber, which was connected to the outlet port of the heating chamber with a T-shaped hollow jointer. Four outlet ports were made in the holding chamber at O1, O2, O3, and O4, respectively, for the holding period of 15, 30, 45, and 60 s. The location of the outlet ports from the bottom end lid were L1, L2, L3, and L4, respectively for 15, 30, 45, and 60 s holding period. The length of the outlet ports from the base/inlet port was determined based on the designed flow rates for respective EFS-temperature combinations. The design dimensions of the isothermal holding chamber are shown in Table 3.1 and Table 4.6, and its schematic diagram is shown in Fig. 3.11. The joints and openings were fastened using Teflon tape to make it leakage-proof during OH operations.

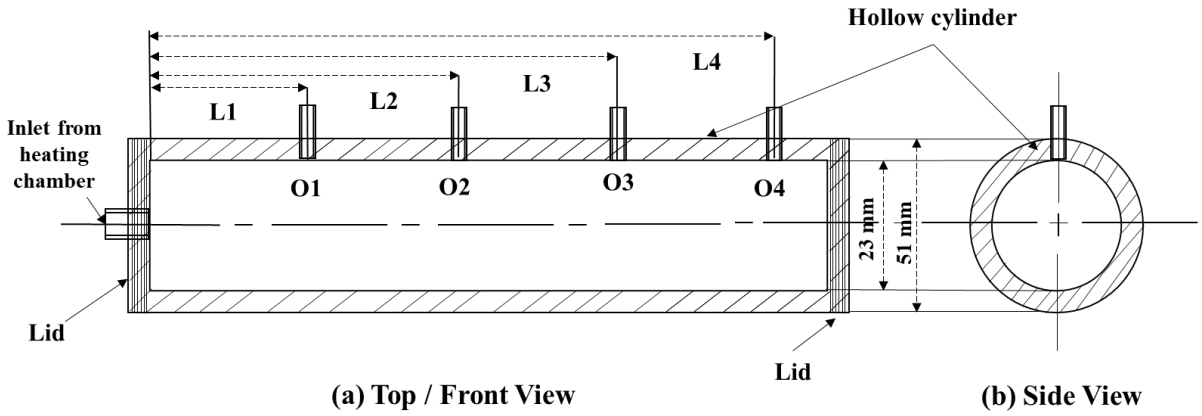

Fig. 3.11 Schematic diagram of an isothermal holding chamber

3.2.2.3.3 Electrodes

During OH, there are chances of metal ions transfer in the food samples from electrodes due to electrophoresis. To restrict such unwanted metal ion transfer in the food samples, a suitable electrode is very much desired. It was found that the platinized titanium electrodes are suitable for the ohmic heating process as they restrict the chances of electric corrosion. Therefore, in the present study, two circular-shaped platinized titanium electrodes were used, as shown in Fig. 3.13(c). The diameter and thickness of the electrodes were 52 mm and 1 mm, respectively (Table 3.1).

3.2.2.3.4 T-shaped jointer port

The outlet port of the heating chamber and inlet port of the isothermal holding chamber were connected with a T-shaped hollow jointer, as shown in Fig. 3.9. Teflon material was used to fabricate the jointer to restrict the heat loss from the fruit juice going to the isothermal holding chamber from the heating chamber. The dimension of the jointer is shown in Table 3.1 and its schematic diagram is shown in Fig. 3.12.

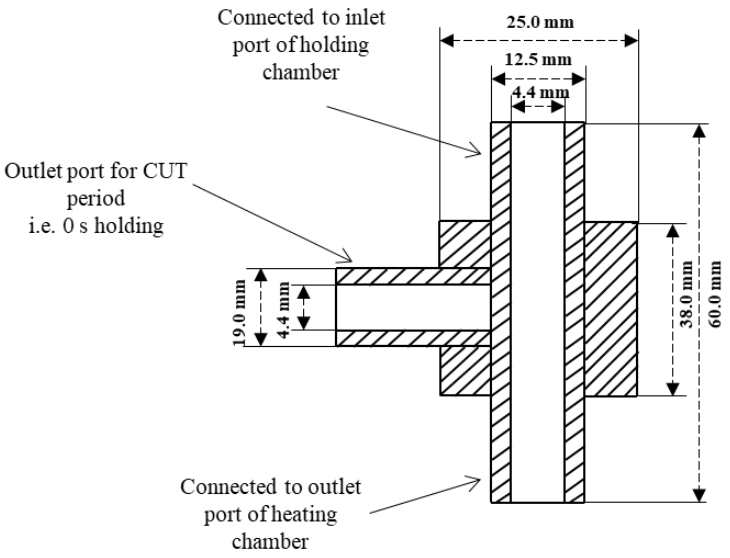

Fig. 3.12 Schematic diagram of a T-shaped hollow jointer

3.2.2.3.5 Power supply and temperature controller

The power supply was supplied to the fruit juice for OH via electrodes and the amount of the voltage was controlled by a variac transformer (D.500, Servokon Systems Ltd.). The transformer used was single phase, 50 Hz with an output voltage range of 0 – 500 V with a maximum current carrying capacity of 30 A. The input to the transformer was a domestic line power supply of 240 V, single phase, and 50 Hz. Therefore, with an electrode–to–electrode gap of 100 mm, the COH system can be designed for the working range of 0 to 45 V/cm EFS. Also, the temperature of the juice during OH was controlled by regulating the power supply through a temperature controller (UTC 4202, Multispan).

3.2.2.3.6 Other accessories

One K-type thermocouple insulated with Teflon tape was placed at the outlet port of the COH section to monitor the outlet temperature of the juice going to the isothermal holding chamber. The juice was pumped into the heating chamber through a peristaltic pump (ENPD 100 Victor, Enertech Electronics Pvt. Ltd.) from an inlet tank. The current and voltage were measured using a multimeter (Fluke 115 True RMS).

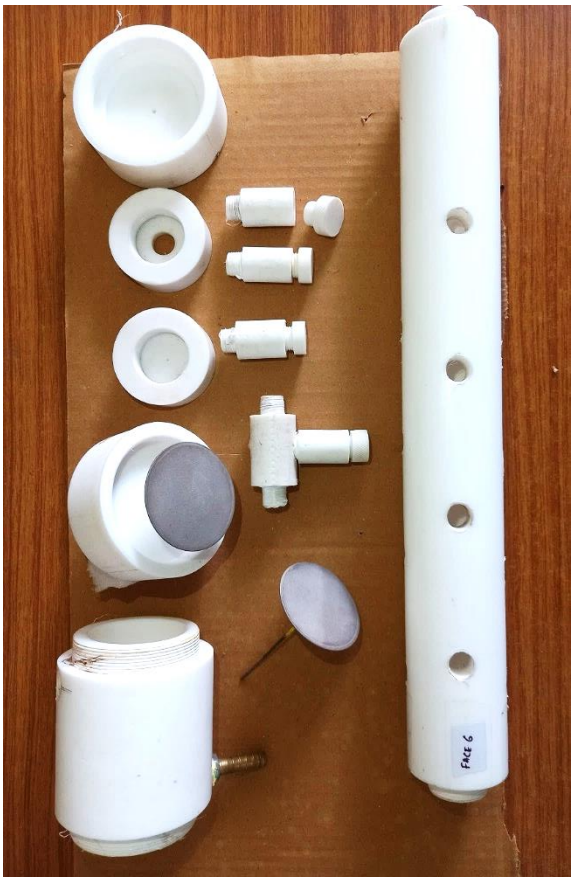

(a)

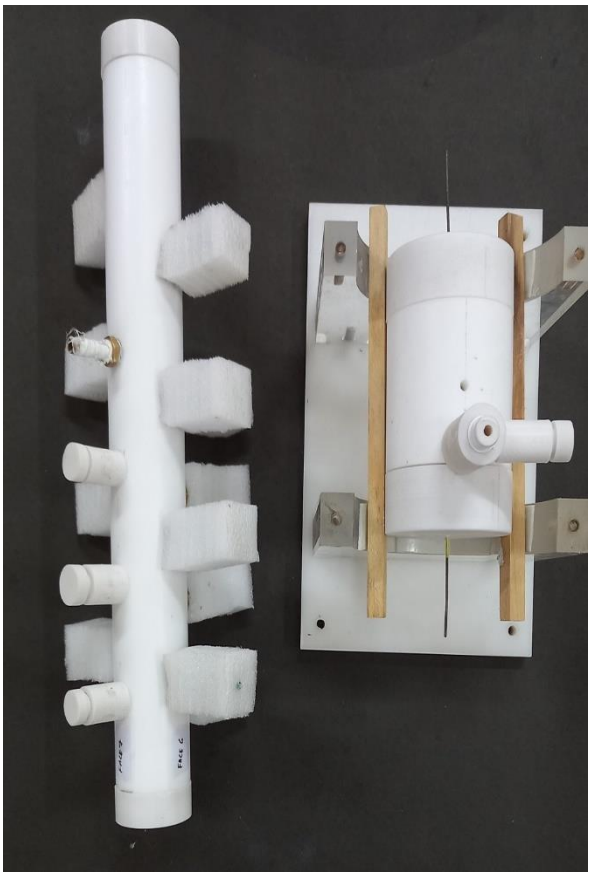

(b)

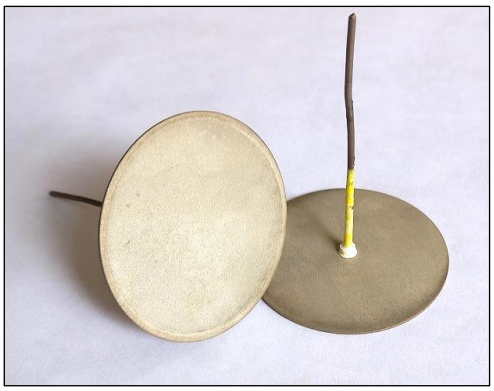

(c)

Fig. 3.13 (a) dissembled parts of heating and isothermal holding chamber of COH system, (b) assembled COH and isothermal holding chamber, and (c) electrodes

Table 3.1 Dimension parameters of COH system

Parameters	Dimension (mm)
Heating Section:	
Outer diameter	75.0
Inner diameter	48.0
Length including lids	131.0
Inlet port	
Location of centre point from the end	18.5
Inner diameter	5.0
Outer diameter	8.5
Outlet port	
Location of centre point from another end	18.5
Inner diameter	4.4
Outer diameter	25.0
Electrodes:	
Diameter	52.0
Thickness	1.0
Electrode-to-electrode gap	100.0
Isothermal holding section:	
Outer diameter	51.0
Inner diameter	23.0
Inlet port	
Inner diameter	4.4
Thread diameter	12.5
Outer diameter	25.0
Outlet port	
Inner diameter	4.4
Thread diameter	12.5
Outer diameter	19.0
T-shaped jointer	
Heating chamber side	
Inner diameter	4.4
Thread diameter	12.5
Outer diameter	25.0
Holding chamber side	
Inner diameter	4.4
Thread diameter	12.5
Outer diameter	25.0
Outlet port for CUT period	
Inner diameter	4.4
Outer diameter	19.0
Total length	60.0

3.2.3 Sample preparation

Fresh fruits (cucumber, orange, pineapple, tomato, and lemon) were purchased from the local market of Tezpur University, Assam, India. The peels, eyes, and core of the pineapples and peels of the oranges and lemons were removed. The edible portions of the fruits were cut into smaller pieces using a sharp knife, and juice was extracted in a juice crusher (Gee Gee Foods & Packaging Co Pvt. Ltd). The extracted juice was filtered using two layered fine muslin cloths. The filtered juice was used to study the heating performance of the lab-scale developed COH system.

To study the heating performance of the standardized juice based on the °Brix/Acid, pineapple juice was selected and standardized to different °Brix/Acid ratios viz., 18, 22, 26 °Brix/Acid (Kumar et al., 2024). The detailed procedure to make the standardized pineapple juice is explained in the Section 3.2.5. To conduct the experiments of Objectives 3, 4, and 5, the pineapple juice was standardized at 22 °Brix/Acid using the same procedure as explained in Section 3.2.5.

3.2.4 Physico-chemical properties

3.2.4.1 Moisture content

The moisture content (MC) was determined by placing 10 mL of the juice in an oven at 105 ± 5 °C for 24 hours or until a constant weight was achieved and was calculated using Eq. 3.1 (Singh et al., 2019).

$$MC\ (\%wb) = \frac{(W_2 - W_1) - (W_3 - W_1)}{(W_2 - W_1)} \quad \text{(Eq. 3.1)}$$

Where W_1, W_2, and W_3 are the weight of empty Petri-plate, Petri-plate with samples, and Petri-plate with dry samples, respectively.

3.2.4.2 pH

The pH was measured by using a pH meter (pH 700, Eutech instruments) after calibrating with a standard pH buffer (pH 4.0, 7.0, and 9.1) at room temperature.

3.2.4.3 Total soluble solids (TSS)

The TSS was measured using a portable hand refractometer (ERB-32, ERMA, Range = 0 to 32 °Brix) at room temperature.

3.2.4.4 Titratable acidity

The titratable acidity (TA, %) was estimated by the titration of 0.05 N NaOH solution against sample juice in the presence of phenolphthalein as an indicator (pH 8.2 as an endpoint) and calculated using Eq. 3.2 (Ranganna, 2001).

$$\%\,TA = \frac{Titre\ (mL) \times Normality \times Volume\ make\ up(mL) \times Equivalent\ weight \times 100}{Volume\ of\ aliqout\ (mL) \times Volume\ of\ sample(mL) \times 1000} \times 100 \quad \text{(Eq. 3.2)}$$

3.2.4.5 Colour parameters

The colour values of the juice were measured in terms of CIE L^* (light to dark), a^* (green to red), and b^* (blue to yellow) scale using Hunter Colour Lab Spectrophotometer (Ultrascan VIS, Hunter Colour Lab, USA). The overall colour change was estimated from Eq. 3.3 (Makroo et al., 2022).

$$\Delta E = \sqrt{(L_o^* - L_t^*)^2 + (a_o^* - a_t^*)^2 + (b_o^* - b_t^*)^2} \quad \text{(Eq. 3.3)}$$

Where, L_o^*, a_o^*, b_o^*, and L_t^*, a_t^*, b_t^* are the colour values of the untreated and treated juice, respectively.

3.2.4.6 Vitamin C

The juice's vitamin C or ascorbic acid content was estimated by following the method suggested by Ranganna (2001). 5.0 mL of juice was made-up to 50.0 mL with 3.0% metaphosphoric acid. An aliquot of 10.0 mL was titrated with 0.025% (w/v) 2,6 dichloroindophenol dye solution until a light pink colour persisted for approximately 15 s. The dye solution was prepared by mixing 62.5 mg of 2,6 dichloroindophenol in approximately 150 mL of hot distilled water containing 52.5 mg of sodium bicarbonate. The solution was cooled, and the volume was made to 250 mL by adding distilled water. The dye solution was stored in refrigerated condition and standardized before use. The standardization was done by titrating it with the 5.0 mL of standard ascorbic acid solution mixed with 5.0 mL of 3.0% metaphosphoric acid. The dye factor was determined in terms of mg of ascorbic acid in 1.0 mL of the dye solution. The vitamin C content in the sample was calculated using Eq. 3.4.

$$Vitamin\ C\ (mg/100\ mL) = \frac{Titre \times volume\ made\ up \times dye\ factor \times 100}{Volume\ of\ aliquot \times volume\ of\ sample} \quad \text{(Eq. 3.4)}$$

3.2.5 Preparation of different °Brix/Acid of pineapple juice

The pineapple juice was removed from -18 °C and thawed at room temperature. The TSS and titratable acidity (TA) were 11.6 ± 0.1 °Brix and 0.974 ± 0.062%, respectively. The juice was standardised at varied °Brix/Acid. The TSS was maintained at 12 °Brix (targeted), and the TA (targeted) was maintained at 0.667, 0.545, and 0.462%, respectively, for 18, 22, and 26 °Brix/Acid. To obtain targeted TSS and TA for the desired °Brix/Acid, mathematical Eq. 3.5, Eq. 3.6, Eq. 3.7, and Eq. 3.8 were used (Kumar et al., 2024).

The total amount of standardised pineapple juice can be determined as:

$$Total\ unit\ of\ SPJ = \frac{TA_{USPJ}\ (\%)}{TA_{SPJ}(\%)} = X \qquad \{For,\ \%TA_{USPJ} > \%TA_{SPJ}\} \qquad (Eq.\ 3.5)$$

Where SPJ and USPJ are standardised pineapple juice and unstandardised pineapple juice, respectively. TA_{USPJ} and TA_{SPJ} are titratable acidity (%) of the USPJ and SPJ, respectively. Therefore, the ratio between USPJ and the required sugar solution becomes:

$$\frac{USPJ\ (mL)}{Sugar\ Solution\ (mL)} = \frac{1}{(X-1)} \qquad (Eq.\ 3.6)$$

The TSS of the required sugar solution to be mixed with USPJ can be determined as follows:

$$\frac{(TSS_{USPJ} \times 1) + \{TSS_{SS} \times (X-1)\}}{X} = TSS_{SPJ} \qquad (Eq.\ 3.7)$$

$$TSS_{SS} = \frac{(TSS_{SPJ} \times X) - (TSS_{USPJ} \times 1)}{(X-1)} \qquad (Eq.\ 3.8)$$

TSS_{SS}, TSS_{USPJ}, and TSS_{SPJ} are the total soluble solids of the required sugar solution, USPJ, and SPJ, respectively. The above equations can be used to standardize fruit juice based on the °Brix/Acid, where the acid content of the juice is higher than the required juice samples.

3.2.6 Heating performance

Electrical conductivity refers to the ability to transport electrical charge across the conducting medium whenever any voltage gradient is introduced. The electrical conductivity and heating rate during OH of samples were calculated as shown in Eq. 3.9 and Eq. 3.10, respectively (Ramaswamy et al., 2014; Sakr and Liu, 2014).

$$\sigma = \frac{L}{A} \times \frac{I}{V} \qquad (Eq.\ 3.9)$$

$$HR = \frac{(T_F - T_I)}{t} \qquad (Eq.\ 3.10)$$

Where σ, L, A, I, and V are the EC (S/m), the gap between electrodes (m), the cross-sectional area of electrodes (m^2), current (A), and voltage (V) across the sample, respectively. HR, T_F, T_I, and t are the heating rate (°C/min), final temperature (°C), initial temperature (°C), and time (min). The system performance coefficient (SPC) is the ratio of the energy utilized to raise the temperature of the juice to the electrical energy supplied. It was calculated to check the energy efficiency of the COH system, as shown in Eq. 3.11 (Sakr and Liu, 2014).

$$SPC = \frac{Energy_{utilised}}{Energy_{supplied}} = \frac{\sum m\, C_p\, \Delta T}{\sum V\, I\, \Delta t} \quad \text{(Eq. 3.11)}$$

Where m, C_p, V, I, and Δt is the cumulative mass of juice in the chamber and mass outflow, specific heat capacity (kJ/kg°C), voltage gradient (V), current (A) and time interval (s), respectively. ΔT is the difference between initial and final temperature. The specific heat (C_p) (kJ/kg°C) of juice was calculated by using Eq. 3.12 in the moisture range of 40-90% wb (Singh et al., 2019).

$$C_p = 1.675 + 0.025\, W \quad \text{(Eq. 3.12)}$$

Where, W is the moisture content (%wb), specific heat was calculated for all four samples (USPJ, 18, 22, and 26 °Brix/Acid), and it was assumed that it would remain constant throughout the ohmic process (i.e., it would not change with temperature).

3.2.7 Enzymes and microbial inactivation

3.2.7.1 Polyphenol oxidase (PPO):

The enzyme extraction solution was prepared in 0.2 M Sorensen's phosphate (SSP) buffer (pH 6.5) that contained 4.0% (w/v) of PVPP, 1.0% (v/v) triton X-100, and 1.0 M NaCl. An equal proportion of the sample and extraction solution was mixed properly, vortexed (bhrmi 1.0, Labquest Borosil) for 240 s, and then centrifuged (Velocity 14R Refrigerated Centrifuge, Dynamica) at 10,000 RCF (relative centrifugal force or g-force) at 4.0 °C for 1800 s. The supernatant was filtered as a crude extract using Whatman no. 01 filter paper (Terefe et al., 2010).

For the assay, 0.2 mL of crude extract was mixed with 1.8 mL of 0.2 M SSP buffer (pH 6.5), and then 1.0 mL of 0.15 M pyrocatechol solution was added. The absorbance was taken immediately at a regular interval of 10 s for 240 s against 0.2 M SSP buffer blank at 420 nm wavelength using a UV-VIS double beam spectrophotometer (Dynamica, Halo DB20S). The absorbance was plotted against time, and the PPO activity was estimated from the initial linear

portion of the curve. Change in 0.001 absorbances per min is termed as 1.0 unit of PPO activity and expressed as % residual activity (%RA) of PPO as shown in Eq. 3.13 where 'A_t' and 'A_i' are the PPO activity at any time 't' and initial activity, respectively (Makroo et al., 2022).

$$\% RA = \frac{Enzyme\ activity\ of\ the\ treated\ samples}{Enzyme\ activity\ of\ the\ fresh\ sample} \times 100 = \frac{A_t}{A_i} \times 100 \quad \text{(Eq. 3.13)}$$

3.2.7.2 Peroxidase (POD):

Enzyme extraction for POD was done similarly to PPO extraction (section 2.6.1). For the assay, 0.28 mL of enzyme extract was mixed with 2.1 mL of 0.05 M SSP buffer and 0.28 mL of 5.0% (w/v) pyrogallol solution in 0.05 M SSP buffer. Then, 0.28 mL of 1.5% (v/v) H_2O_2 solution was added, and absorbance was taken immediately at 485 nm at a regular interval of 10 s for 240 s against a reagent blank using a UV-VIS double beam spectrophotometer (Halo DB20S, Dynamica). The absorbance was plotted against time, and the POD activity was estimated from the initial linear portion of the curve. The %RA of the POD was calculated using Eq. 3.13.

3.2.7.3 Bromelain activity:

1 mL of juice was mixed with 2.0 mL of extraction solution made of 5.0 mM of EDTA and 25.0 mM cysteine freshly prepared in 0.1 M sodium phosphate buffer maintained at pH 8.0. It was vortexed for 3.0 min and then centrifuged at 10,000 g at 4 °C for 30 min. The supernatant was filtered and used as fresh crude enzyme extract. Assay was done using 0.2 mL crude extract mixed properly with 2.2 mL of 1.0% (w/v) casein solution prepared in 0.1 M glycine sodium hydroxide buffer maintained at pH 8.7, which contained 25.0 mM cysteine. The mixture was incubated for 15 min at 37 °C. The reaction was stopped by adding 3.6 mL of 5.0% TCA, centrifuged at 5,000 g for 5 min, and filtered through Whatman no. 01 filter paper. Absorbance was taken at 280 nm against reagent blank, and the residual activity (RA, %) was calculated using Eq. 3.13 (Chakraborty et al., 2015).

3.2.7.4 Total microbial load:

Spread plate method was used in which a solution of 2.8% (w/v) nutrient agar media and 0.85% (w/v) saline were freshly prepared in distilled water. An approximately 12.0 – 15.0 mL of the sterilized media was poured in the sterilized petri-plates and kept in a laminar flow undisturbed to solidify. Samples were serially diluted in 0.85% (w/v) sterilised saline water. Inoculation was done using 0.1 mL sample and incubated at 37 °C for 48 hours. Number of colonies forming units were recorded and the total number of microorganism present in the samples was calculated using the Eq. 3.14 (Ranganna, 2001).

$$N = \frac{N_c}{V_s \times DF} \quad \text{(Eq. 3.14)}$$

Where, N is the number of microorganisms present in the sample (CFU/mL), N_c is the number of colonies formed in the petri-plates, V_s is inoculation volume and DF is the serial dilution factor.

3.2.8 Inactivation kinetic modelling:

Any thermal or COH system for juice processing consists of three main steps: heating (CUT period), isothermal holding, and cooling. Taking out samples during the heating period to study inactivation kinetics is difficult as the temperature changes very fast. So, the inactivation of the enzyme is divided into two parts, i.e., (A_o/A_i) at the end of the CUT period and (A_t/A_o) during the isothermal holding. The inactivation kinetics was done during isothermal treatment, i.e., A_t/A_o, where 0 s holding time was taken as the initial value (A_o). Eq. 3.15 shows the overall enzyme inactivation where A_t, A_i, and A_o are the enzyme activity at any time 't,' untreated juice, and at the CUT period, respectively (Chakraborty et al., 2015).

$$\frac{A_t}{A_i} = \left(\frac{A_o}{A_i}\right) \times \left(\frac{A_t}{A_o}\right) \quad \text{(Eq. 3.15)}$$

3.2.8.1 Enzyme inactivation kinetic modelling:

The enzyme activity was determined at every 15 s interval up to 60 s (in the holding section) and used to study five different kinetic models for PPO and POD inactivation viz., first order, distinct isozymes, fractional conversion, Weibull distribution, and sigmoidal logistic model. These models were selected to understand the behaviour of PPO and POD inactivation under present treatment conditions. The first-order kinetic model was chosen because of its simplicity and practical to use as it assumes one-step irreversible breaking of bond or structure during thermal treatment and has a linear relationship between enzyme activity and time (Terefe et al., 2010). But enzymes like PPO and POD often exist in multiple isozyme variants with distinct biochemical properties and thermal stability, so using a distinct isozyme kinetic model will allow for a more tailored representation of the inactivation kinetics for each isozyme and helps in understanding how different variants contribute to the overall inactivation process (Brochier et al., 2016). Meanwhile, the fractional conversion model aligns with the biological reality that enzyme inactivation is often a multi-step process. On the other hand, the Weibull distribution model is flexible and can describe a wide range of shapes for inactivation curves as the enzyme inactivation process may exhibit a non-linear pattern that cannot be accurately represented by simple first-order kinetics, thus making it suitable for capturing diverse pattern observed in

enzyme inactivation. The tail behaviour of the PPO and POD may also be captured by the Weibull model when inactivation kinetics exhibit non-exponential behaviour over time (Shalini et al., 2008). On some occasions, enzyme inactivation exhibits different phases like initial lag phases, a rapid inactivation phases, and a final plateau phase. This makes the logistic model suitable, which is characterised by an S-shaped curve often observed in enzyme inactivation. The logistic model can represent the saturation effect in enzyme inactivation, indicating that the inactivation process gradually slows down as it approaches complete inactivation. This is relevant for enzymes like PPO and POD, where the inactivation rate may decrease over time.

On the other hand, three kinetic models viz., first order, Weibull distribution, and logistic models were used for bromelain inactivation because of its highly thermal sensitivity.

The first-order kinetic model for enzyme inactivation during thermal treatment is shown in Eq. 3.16, where 'k' is the rate constant (min^{-1}) and 't' is the treatment time (min) (Terefe et al., 2010).

$$\frac{A_t}{A_o} = \exp(-k \times t) \quad \text{(Eq. 3.16)}$$

The distinct isozymes kinetic model for enzyme inactivation is shown in Eq. 3.17, where 'A_L' and 'A_s' are the thermally labile and thermally stable fractions, respectively. Also, 'k_L' and 'k_s' are the reaction rate constants (min^{-1}) for the thermal labile and thermal resistant fractions, respectively (Brochier et al., 2016).

$$\frac{A_t}{A_o} = A_L \exp(-k_L \times t) + A_s \exp(-k_s \times t) \quad \text{(Eq. 3.17)}$$

The presence of highly heat-resistant fractions and a non-zero activity was considered in a first-order kinetic model. Thus, a fractional conversion model was used, as shown in Eq. 3.18 (Shalini et al., 2008).

$$\frac{A_t}{A_o} = A_r + \{(A_o - A_r) \times \exp(-K \times t)\} \quad \text{(Eq. 3.18)}$$

Sometimes, the inactivation takes place continuously upon thermal treatment and can be best described by applying the Weibull distribution model, which includes two factors viz., scale factor (δ, min) and shape factor (n) as shown in Eq. 3.19. The shape factor 'n' represents the shape of the fitted curve, whether it is concave ($n < 1$), convex ($n > 1$), or linear ($n = 1$), depending on the numerical value of the 'n.' So, the Weibull model is a robust curve-fitting tool that provides a better-predicting model (Shalini et al., 2008).

$$\frac{A_t}{A_o} = \exp\left[-\left(\frac{t}{\delta}\right)^n\right] \quad \text{(Eq. 3.19)}$$

In addition to the above models, a sigmoidal logistic model was also used for the inactivation kinetics to investigate different phases of enzyme inactivation, as shown in Eq. 3.20 (Pipliya et al., 2022).

$$RA = \frac{1-A_{min}}{1+\left(\frac{t}{t_{50}}\right)^P} + A_{min} \quad \text{(Eq. 3.20)}$$

Where 'RA' is the residual activity, 'A_{min}' is the lowest value (≥ 0) of RA of enzymes, 'P' is the power term, and 't_{50}' is the time for half residual activity.

3.2.8.2 Microbial inactivation kinetic modelling:

The first-order kinetic model for microbial inactivation during thermal treatment is shown in Eq. 3.21, where 'k' is the rate constant (min^{-1}) and 't' is the treatment time (min) (Chen, 2007).

$$Log\left(\frac{N_t}{N_o}\right) = -\left(\frac{k}{2.303}\right) \times t \quad \text{(Eq. 3.21)}$$

The Weibull distribution model for microbial inactivation during thermal treatment is shown in Eq. 3.22, where, 'δ' (min) is scale factor and 'n' is shape factor (Pereira et al., 2020).

$$Log\left(\frac{N_t}{N_o}\right) = -\left(\frac{t}{\delta}\right)^P \quad \text{(Eq. 3.22)}$$

The modified Gompertz model for microbial inactivation during thermal treatment is shown in Eq. 3.23 (Shao et al., 2019).

$$Log\left(\frac{N_t}{N_o}\right) = -A \times exp\left\{-exp\left[\frac{K_{max} \times \exp(1)}{A} \times (t_s - t) + 1\right]\right\} \quad \text{(Eq. 3.23)}$$

3.2.8.3 Vitamin C degradation kinetic modelling:

The vitamin C degradation kinetic modelling was studied using first-order, Weibull distribution, and logistic models, as shown in Eq. 3.16, Eq. 3.19, and Eq. 3.20, respectively.

3.2.8.4 Decimal reduction time and activation energy

The decimal reduction time (D-value) can be calculated from Eq. 3.24, where 'k' is the rate constant (min^{-1}) (Castro et al., 2004).

$$D - value = \frac{2.303}{k} \quad \text{(Eq. 3.24)}$$

The activation energy (E_a) can be calculated from Eq. 3.25, where K_1 (min) and K_2 (min) are rate constant at temperatures T_1 (°C) and T_2 (°C). E_a and R are activation energy and universal gas constant (Icier et al., 2008).

$$ln\frac{K_2}{K_1} = -\frac{E_a}{R}\left(\frac{1}{T_2} - \frac{1}{T_1}\right) \quad \text{(Eq. 3.25)}$$

3.2.8.5 Kinetic modelling during storage study

The kinetic modelling of vitamin C degradation, enzyme (PPO, POD, bromelain) degradation, and microbial growth was examined with zero-order (Eq. 3.26), first-order (Eq. 3.16), and second-order (Eq. 3.27) model.

$$A_t - A_o = -k_o t \quad \text{(Eq. 3.26)}$$

$$\frac{1}{A_t} - \frac{1}{A_o} = k_2 t \quad \text{(Eq. 3.27)}$$

3.2.8.6 Goodness of fit parameters

The R^2, SSE, RMSE, residuals, and R_d are shown in Eq. 3.28, Eq. 3.29, Eq. 3.30, Eq. 3.31, and Eq. 3.32, respectively (Brochier et al., 2016).

$$R^2 = 1 - \frac{\sum_{i=1}^{n}(Y_i - Y_p)^2}{\sum_{i=1}^{n}(Y_i - Y_a)^2} \quad \text{(Eq. 3.28)}$$

$$SSE = \sum_{i=1}^{n}(Y_i - Y_p)^2 \quad \text{(Eq. 3.29)}$$

$$RMSE = \sqrt{\frac{\sum_{i=1}^{n}(Y_i - Y_p)^2}{n}} \quad \text{(Eq. 3.30)}$$

$$Residuals = (Y_i - Y_p) \quad \text{(Eq. 3.31)}$$

$$R_d = \frac{100}{n} \times \sum_{i=1}^{n}\frac{|Y_i - Y_p|}{Y_i} \quad \text{(Eq. 3.32)}$$

where 'Y_i' is the observed value, 'Y_p' is the predicted value, 'Y_a' is the average observed value, and 'n' is the number of observations.

3.2.8.7 Model validation and performance:

The accuracy factor (A_f) and bias factor (B_f) were studied for the validation and performance capabilities of the models using Eq. 3.33 and Eq. 3.34, respectively. The 'A_f' indicates how close the simulations are to the observations (Pipliya et al., 2022; Vega et al., 2016).

$$A_f = 10^{\sum_{i=1}^{n}|log(Y_p/Y_i)|/n} \quad \text{(Eq. 3.33)}$$

$$B_f = 10^{\sum_{i=1}^{n}\{log(Y_p/Y_i)\}/n} \quad \text{(Eq. 3.34)}$$

3.2.8.8 Akaike information criteria for model selection

Akaike information criteria (AIC) are used to discriminate, rank, and choose the best model among several competing models, as shown in Eq. 3.35.

$$AIC = m\ln(SSE) - m\ln(m) + 2j \quad \text{(Eq. 3.35)}$$

where 'm' is the number of observations, 'SSE' is the residual sum of square error, and 'j' is the number of model parameters. Akaike increment (Δ_i), as shown in Eq. 3.36, where AIC_{min} corresponds to the best-fit model with the least AIC value. The Δ_i values are simplistic and permit easy interpretation, comparison, and ranking of several competing models (Pipliya et al., 2022; Vega et al., 2016).

$$\Delta_i = AIC_i - AIC_{min} \quad \text{(Eq. 3.36)}$$

3.2.9 Statistical analysis

IBM SPSS 23.0 software was used for statistical analysis at a significance level of 5.0%. Also, the Tukey HSD test was conducted at a significance level of 5.0% to check the mean significant differences. Kinetic modeling was done with MATLAB R2015a. Statistical parameters like goodness of fit (R^2, RMSE, SSE, residuals, and R_d), model validation (A_f, and B_f), and AIC were calculated using Microsoft Excel 2019.